The ectomycorrhizal fungus *Pisolithus microcarpus* encodes a microRNA involved in cross-kingdom gene silencing during symbiosis

Johanna Wong-Bajracharya[a,b], Vasanth R. Singan[c], Remo Monti[c], Krista L. Plett[a,b], Vivian Ng[c], Igor V. Grigoriev[c,d], Francis M. Martin[e], Ian C. Anderson[a], and Jonathan M. Plett[a,1]

[a]Hawkesbury Institute for the Environment, Western Sydney University, Richmond, NSW 2753, Australia; [b]NSW Department of Primary Industries, Elizabeth Macarthur Agricultural Institute, Menangle, NSW 2568, Australia; [c]US Department of Energy Joint Genome Institute, Lawrence Berkeley National Laboratory, Berkeley, CA 94720; [d]Plant and Microbial Biology Department, University of California Berkeley, Berkeley, CA 94720; and [e]French National Research Institute for Agriculture, Food and Environment (INRAE), Interactions Arbres/Microorganismes, Laboratory of Excellence ARBRE, 54280 Champenoux, France

Edited by Giles Oldroyd, Crops Science Centre, University of Cambridge, Cambridge, United Kingdom; received February 22, 2021; accepted November 17, 2021

Small RNAs (sRNAs) are known to regulate pathogenic plant–microbe interactions. Emerging evidence from the study of these model systems suggests that microRNAs (miRNAs) can be translocated between microbes and plants to facilitate symbiosis. The roles of sRNAs in mutualistic mycorrhizal fungal interactions, however, are largely unknown. In this study, we characterized miRNAs encoded by the ectomycorrhizal fungus *Pisolithus microcarpus* and investigated their expression during mutualistic interaction with *Eucalyptus grandis*. Using sRNA sequencing data and in situ miRNA detection, a novel fungal miRNA, *Pmic_miR-8*, was found to be transported into *E. grandis* roots after interaction with *P. microcarpus*. Further characterization experiments demonstrate that inhibition of *Pmic_miR-8* negatively impacts the maintenance of mycorrhizal roots in *E. grandis*, while supplementation of *Pmic_miR-8* led to deeper integration of the fungus into plant tissues. Target prediction and experimental testing suggest that *Pmic_miR-8* may target the host NB-ARC domain containing transcripts, suggesting a potential role for this miRNA in subverting host signaling to stabilize the symbiotic interaction. Altogether, we provide evidence of previously undescribed cross-kingdom sRNA transfer from ectomycorrhizal fungi to plant roots, shedding light onto the involvement of miRNAs during the developmental process of mutualistic symbioses.

effector | small RNA | symbiosis | mycorrhizae | plant defense

Noncoding small RNAs (sRNAs) regulate vital biological processes in a wide range of organisms by regulating gene expression in a highly specific fashion. Despite their short length (usually 20 to 30 nucleotides long), these sRNAs target messenger RNA by complementary base pairing, in which they alter protein production through posttranscriptional gene silencing and translational gene silencing (1). In exceptional cases, they may also activate gene expression (2). Among the different classes of sRNA, microRNAs (miRNAs) are one of the most well-characterized. Precursor miRNAs form self-complementary, hairpin-like stem loop structures [70 to 200 nucleotides long; (3)] that are then diced into short, mature miRNA by DICER-like (DCL) proteins [21 to 24 nucleotides long; (4)]. These miRNAs can then interfere with the expression of their target transcript by cleavage or inactivation when incorporated into an RNA-induced silencing complex together with the ARGONAUT protein AGO1 (5). sRNAs, including miRNAs, have been identified as playing endogenous roles in regulating physiological processes in various fungi, including saprotrophic species [e.g., *Neurospora crassa*; (6)], pathogenic fungi [e.g., *Magnaporthe oryzae*; (7)], and mutualistic fungi [e.g., *Rhizophagus irregularis*; (8)]. Another class of mutualistic fungi, the ectomycorrhizal (ECM) fungi, are also presumed to produce miRNAs, as they possess the necessary components for the sRNA synthesis pathway, including AGO proteins, DCL proteins, and RNA-dependent RNA polymerases (6, 9–12).

ECM fungi form essential, nutrient-acquiring symbioses with the roots of most temperate and boreal forest trees (13). Evolved from multiple lineages of saprotrophic ancestors, ECM fungi exhibit conserved genomic alterations that are thought to have led to their ability to colonize host tissues (14). One mechanism in particular includes the encoding of effector-like signaling proteins (15). To date, only a small number of these have been characterized, but their base mode of action appears to be to alter host signaling and metabolism to foster the early stages of symbiosis (16–20). sRNAs may be another signaling molecule used by ECM fungi during symbiosis. Proof of miRNAs regulating fungal–plant interactions have been experimentally shown in pathogenic models, whereby small interfering RNAs (siRNAs) produced by the fungal pathogen *Botrytis cinerea* were found to be exported into *Arabidopsis* leaves, binding to the host AGO1 protein and suppressing host immunity by targeting MAPK genes (21). Emerging evidence suggests similar cross-kingdom sRNA transfer, and silencing occurs in other plant pathosystems involving various fungal

Significance

Plant genomes encode hundreds of genes controlling the detection, signaling pathways, and immune responses necessary to defend against pathogens. Pathogens, in turn, continually evolve to evade these defenses. Small RNAs, such as microRNAs (miRNAs), are one mechanism used by pathogens to overcome plant defenses and facilitate plant colonization. Mounting evidence would suggest that beneficial microbes, likewise, use miRNAs to facilitate symbiosis. Here, we demonstrate that the beneficial fungus *Pisolithus microcarpus* encodes a miRNA that enters plant cells and stabilizes the symbiotic interaction. These results demonstrate that beneficial fungi may regulate host gene expression through the use of miRNAs and sheds light on how beneficial microbes have evolved mechanisms to colonize plant tissues.

Author contributions: J.W.-B., K.L.P., I.C.A., and J.M.P. designed research; J.W.-B., V.R.S., R.M., K.L.P., F.M.M., and J.M.P. performed research; V.N., I.V.G., I.C.A., and J.M.P. contributed new reagents/analytic tools; J.W.-B., V.R.S., R.M., K.L.P., V.N., I.V.G., F.M.M., I.C.A., and J.M.P. analyzed data; and J.W.-B., V.R.S., K.L.P., I.V.G., F.M.M., I.C.A., and J.M.P. wrote the paper.

The authors declare no competing interest.

This article is a PNAS Direct Submission.

[1]To whom correspondence may be addressed. Email: j.plett@westernsydney.edu.au.

This article contains supporting information online at http://www.pnas.org/lookup/suppl/doi:10.1073/pnas.2103527119/-/DCSupplemental.

Published January 10, 2022.

pathogens [e.g., *Verticillium dahliae*, *Blumeria graminis*, and *Scleotinia sclerotiorum*; (22–25)]. Besides fungal pathogens, a recent report also demonstrated that the sRNAs produced by mutualistic rhizobia regulate nodulation by hijacking the host AGO1-dependent RNA interference machinery (26). Furthermore, in silico analyses predict that sRNA produced by mutualistic arbuscular mycorrhizal (AM) fungi may target gene expression in host plants (18, 27). Despite the lack of experimental characterization of the miRNAs, this latter study supports the concept that cross-kingdom sRNA silencing is more broadly applicable beyond pathogenic models to mutualistic plant–fungal interactions.

In this current study, we made use of the mutualistic ECM fungus *Pisolithus microcarpus* and its interaction with the roots of the host plant *Eucalyptus grandis* to better understand the putative role of fungal, miRNA-mediated gene regulation during ECM symbiosis. Genome mining and sRNA sequencing (sRNA-seq) was performed at different developmental stages of mycorrhizal root tip formation to identify fungal miRNAs differentially regulated during ECM colonization. Furthermore, we tested the potential existence of cross-kingdom sRNA transfer between *P. microcarpus* and *E. grandis*. We give evidence here supporting the importance of certain miRNAs in cross-kingdom signaling during ECM symbiosis establishment.

Results

Identification and Differential Expression Profiling of *Pisolithus* miRNAs during Root Colonization. The *P. microcarpus* reference genome and sRNA-seq were used to identify fungal miRNAs and examine their expression patterns during ECM colonization. Prediction of miRNA using the ShortStack application identified 11 fungal miRNAs [Table 1; (28)]. These fungal miRNAs exhibited significant differential expression patterns between the different time points of ECM colonization considered, six of which were induced by the colonization process (*Pmic_miR-1*, *Pmic_miR-5*, *Pmic_miR-6*, *Pmic_miR-7*, *Pmic_miR-8*, and *Pmic_miR-10*; Fig. 1 *A* and *B*), expression patterns that were verified using qPCR (*SI Appendix*, Fig. S1). Expressions of some miRNAs were consistent across the time points taken; *Pmic_miR-1* was consistently induced throughout mycorrhizal root tip development, compared to axenically grown fungal colonies, while *Pmic_miR-6* was most highly induced during the early stages of colonization and steadily reduced in expression in the latter stages of colonization (Fig. 1 *A* and *B*). While most of the other identified miRNAs were repressed during colonization, the expression of *Pmic_miR-8* was initially repressed followed by induction at the 2-wk time point, when ingrowth of the mycorrhizal fungus into the root apoplastic space has occurred.

***Pisolithus* Fungal miRNAs Can Be Recovered in *E. grandis* Root Cells during Presymbiosis, prior to Physical Contact.** As certain sRNAs have previously been demonstrated to be secreted from fungal hyphae and taken up into plant cells (21), we similarly tested if we could recover *P. microcarpus* miRNAs in the root cells of *E. grandis*. Using a presymbiotic interaction experimental setup that physically separates the host roots and fungal mycelial tissues but contains pores that allow for the transfer of signaling molecules (Fig. 1*C* and *SI Appendix*, Fig. S2*A*), we found that ~20% of the aligned reads sequenced from the root tissue (679,733 reads in total; Dataset S1) were encoded by the *P. microcarpus* genome instead of *E. grandis*. It is unlikely that these sequences are due to fungal contamination as the membrane used to separate the two organisms was not ruptured by the fungus (Fig. 1*D* and *SI Appendix*, Fig. S2 *B* and *C*). This indicated the possibility that a significant amount of *P. microcarpus* sRNAs are secreted and can be transferred into the cells of a host during root colonization. The majority of these fungal sequences (643,534 reads in total) represent 4,370 sRNA-forming loci in *P. microcarpus* genome (Dataset S2), accounting for 94.7% of all fungal reads. According to the ShortStack sRNA analysis result, most of these sRNA-forming loci (3,993 clusters) produce sRNA between 20 and 24 nucleotides in length and potentially belong to sRNA classes other than miRNAs [Dataset S3; (29)]. Within these sequence clusters, we also found four sequences corresponding to the aforementioned, putative, fungal miRNAs: *Pmic_miR-2*, *Pmic_miR-3*, *Pmic_miR-8*, and *Pmic_miR-9* (Fig. 1*E*). The presence of these transcripts was independently verified using qPCR analysis of RNA extracted from presymbiotic roots (*SI Appendix*, Fig. S3). Based on its high accumulation in plant tissues, we sought to localize *Pmic_miR-8* in plant tissues using fluorescence in situ hybridization (ISH) assays. No immunolocalization signal was detected in presymbiotic *E. grandis* root cells when a no-probe control was performed (Fig. 1*F*) nor was there any signal identified in axenically grown *E. grandis* roots when an anti–*Pmic-miR-8* probe was used (Fig. 1*G*). *Pmic-miR-8* was localized, however, as both a faint haze and as punctate structures in the cells of *E. grandis* roots after presymbiotic contact with the fungus (Fig. 1*I*). In contrast, no fluorescent signals were detectable in similarly treated roots when a scrambled probe was used (Fig. 1*H*). To ensure that the immunolocalization signal was not due to accumulation of *Pmic-miR-8* on the outside of the roots, *E. grandis* roots in presymbiotic contact with *P. microcarpus* were treated with ribonuclease (RNase) for 15 min prior to fixation and immunolocalization. These roots also exhibited the same *Pmic-miR-8* localization (Fig. 1*K*). This signal disappeared, however, when the tissues were treated with RNase postfixation and cell permeabilization (Fig. 1*M*). To further confirm that *Pmic_miR-8* was in the cytoplasm, we plasmolysed another

Table 1. Summary of the putative fungal miRNAs identified with the *P. microcarpus* 441 genome

miRNA name	Locus (chromosome:start-end)	Strand	Predicted precursor length (nt)	Mature miRNA sequence (5′-3′)
Pmic_miR-1	Pis_scaffold_12:478925–479041	—	117	GUUGAGCCUGAUACAGUAGCCU
Pmic_miR-2	Pis_scaffold_16:167685–167760	+	76	UCACUUUCCGAGCUUGUAGUCCAACU
Pmic_miR-3	Pis_scaffold_27:55536–55633	—	98	CGGGUCUGAUGAUGCAGAGUCGGGC
Pmic_miR-4	Pis_scaffold_5:542437–542560	+	124	UAUGGGCUGGCCUAGGCAUGG
Pmic_miR-5	Pis_scaffold_57:72308–72667	+	360	UACCGAUCUGCCUGUGGGACA
Pmic_miR-6	Pis_scaffold_134:66475–66733	—	259	AACGGAUAGAUCAAUAUUAAGACC
Pmic_miR-7	Pis_scaffold_106:26653–26727	+	75	UCCAGCAAGGGGGAAUGGGCU
Pmic_miR-8	Pis_scaffold_237:46412–46486	—	75	UAUUCUCUCCUUGACUUCCC
Pmic_miR-9	Pis_scaffold_502:13132–13222	+	91	UGAACGUGCGUCGUCCAUGCCC
Pmic_miR-10	Pis_scaffold_74:80881–80965	.	85	UCAUCCUCGAACAAGACCUG
Pmic_miR-11	Pis_scaffold_343:1277–1351	+	75	CUUUAUCUCUCGAACGCUGCUGGA

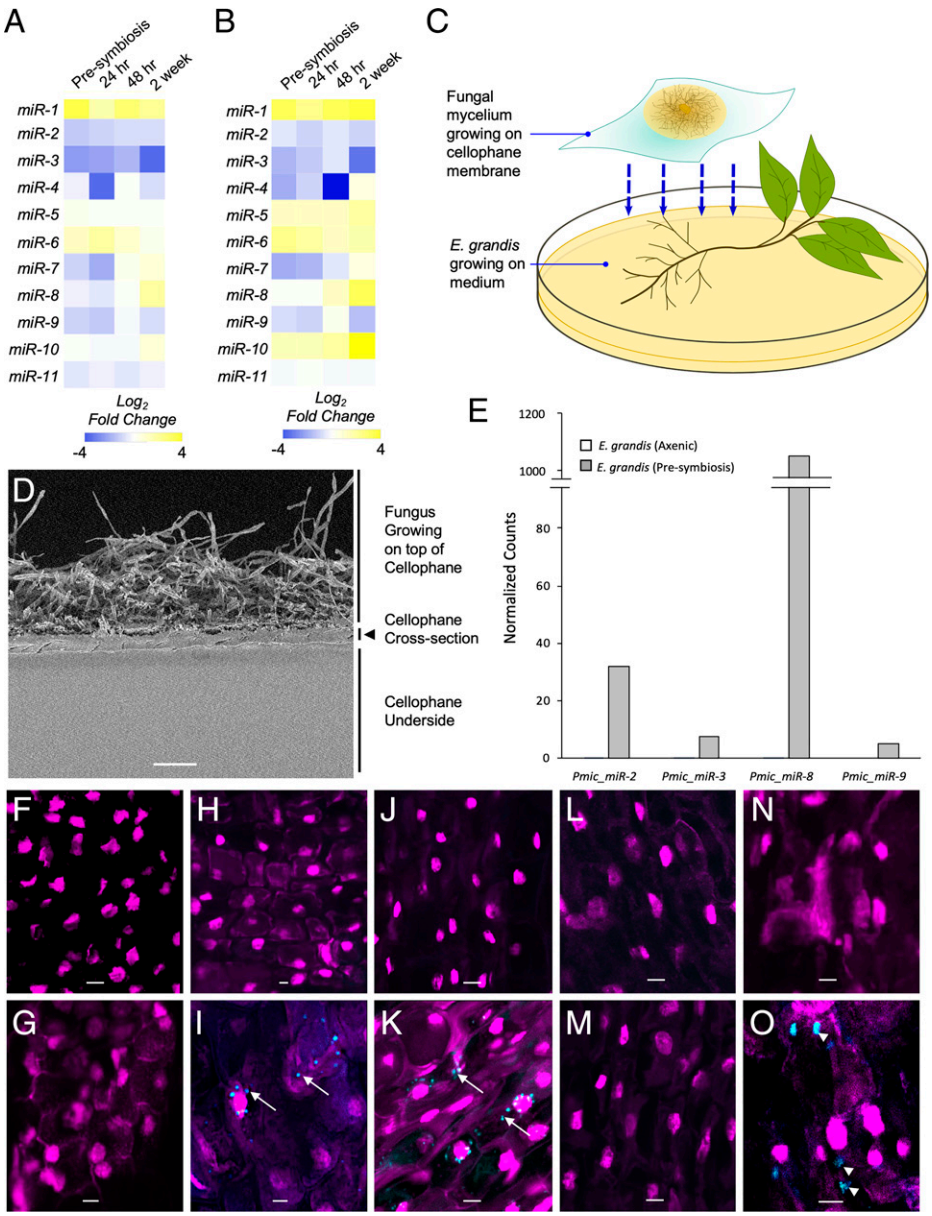

Fig. 1. *P. microcarpus* miRNAs are differentially regulated during ECM symbiosis developments with *E. grandis* roots certain of which can be recovered and localized in the cells of *E. grandis*. Heatmaps showing the fold change in expression of the 11 predicted fungal miRNAs in *P. microcarpus* isolate SI14 (*A*) and isolate SI9 (*B*) across a time course of colonization with *E. grandis* roots. The color scale represents the normalized Log_2 fold change of each miRNA at each timepoint of colonization compared to axenically grown fungal cultures ($n = 3$ to 4). (*C*) Diagram of Petri dish setup for presymbiotic exposure of the two organisms. The fungus is grown on top of a cellophane membrane and then transferred to rest over top of *E. grandis* roots. (*D*) Scanning electron micrograph of a cross-section of the cellophane membrane utilized, showing microscopic pores running throughout the material. (Scale bar, 40 μm.) (*E*) Bar graph depicting normalized read counts of four putative fungal miRNAs detected in *E. grandis* roots after presymbiotic interaction with *P. microcarpus* (presymbiosis; gray bars) but below detection limit in sRNA-seq libraries of *E. grandis* axenically grown roots where no fungus is present (axenic; white bars; see also *SI Appendix*, Fig. S3 for verification of results by qPCR). (*F–O*) ISH localization of *Pmic_miR-8* in *E. grandis* root cells and controls using either a fluorescent anti-*Pmic_miR-8* or scrambled sequence probe (blue signal in images) whereby the nuclei of root cells were visualized with propidium iodide (magenta signal in images). The specific treatments are as follows: probe-free ISH of presymbiotic roots (*F*); ISH of *Pmic_miR-8* in *E. grandis* cells grown axenically (*G*); ISH of presymbiotic roots using a scrambled probe (*H*); ISH of presymbiotic roots using a *Pmic_miR-8* probe with a positive signal for the target found in punctate structures within the cell (arrows) as well as more diffusely throughout the cell (*I*); ISH of presymbiotic roots treated with RNase prior to fixation to remove any RNA adherent to the cell surface and then probed with a scrambled probe (*J*); ISH of presymbiotic roots treated with RNase prior to fixation using a *Pmic_miR-8* probe with a positive signal for the target found in punctate structures within the cell (arrows) (*K*); ISH with a scrambled probe of presymbiotic roots treated with RNase prior to, and post, fixation to remove any RNA adherent to the cell surface and within the cell postpermeabilization (*L*); ISH of presymbiotic roots treated with RNase prior to, and post, fixation to remove any RNA adherent to the cell surface and within the cell postpermeabilization and then probed with a *Pmic_miR-8* probe (*M*); ISH of presymbiotic roots treated to induce plasmolysis using a scrambled probe (*N*); and ISH of presymbiotic roots treated to induce plasmolysis using a *Pmic_miR-8* probe with a positive signal for the target found in larger concentrations within the cell (arrow head) (*O*). All images were acquired using an inverted Leica TCS SP5 laser-scanning confocal microscope with the same settings. (Scale bar, 20 μm for *F–O*.) All images are representative of four biological replicates.

subset of the same roots prior to fixation and immunolocalization and found *Pmic-miR-8* localization in larger, diffuse areas within the cell, supporting the finding that *Pmic-miR-8* is within the cytoplasm of the plant cell (Fig. 1*O*). Overall, the detection of fungal sRNA in *E. grandis* root cells demonstrates the potential existence of sRNA trafficking from the fungus to the host in ECM interactions.

Fungal miRNA *Pmic_miR-8* Stabilizes ECM Colonization. The expression pattern of *Pmic_miR-8* during colonization prompted further characterization of the effect this fungal miRNA has on ECM fungi–root interaction. Four synthetic sRNAs were generated and used to artificially modulate the levels of *Pmic_miR-8* in vitro in two ways: 1) double-stranded (ds) and single-stranded, mature *Pmic_miR-8* RNA was used to increase the overall level of this miRNA in tissues during colonization and 2) antisense (as) *Pmic_miR-8* with a Zen-modification (*asZEN*) and *asPmic_miR-8* designed with a bulge (*asBulge*) at bases 10 and 11 were used to "inhibit" the action of the mature *Pmic_miR-8* miRNA molecules through locking the mature miRNA in a ds form unable to be loaded into the ARGONAUT complex. As controls to these treatments, we used scrambled miRNA (*ssScrambled*) and a scrambled miRNA inhibitor (*asScrambled*) sequence as well as *ssPmic_miR-8**, which is the complementary sequence to the mature miRNA and not expected to be active. The application of *ss* and *dsPmic_miR-8* led to increases in detectable *Pmic_miR-8* transcripts in colonized root tissues ($P < 0.05$; Fig. 2*A* and *SI Appendix*, Fig. S4*A*), while *Pmic_miR-8* inhibitor treatments led to a trend toward reduced recovery of *Pmic_miR-8* sequences (Fig. 2*A* and *SI Appendix*, Fig. S4*A*). All control treatments, as well as supplementation of either ss*Pmic_miR-8* or ds*Pmic_miR-8*, led to the normal formation of mycorrhizal root tips (Fig. 2*B*). Treatment with either the *asZen* or *asBulge* inhibitors, however, resulted in regrowth of the root after the initial formation of a mantle in >20% of roots (Fig. 2*C*, white arrows). We considered these latter structures to be senesced mycorrhizal root tips. Statistical analysis of mycorrhizal root tip formation, and of colonized root senescence, found that treatment with either *Pmic_miR-8* inhibitors led to a significant reduction in colonized root tips (Fig. 2*D*; $P < 0.05$). This reduction in colonized roots was almost completely due to the increase in roots that continued to grow after the initial formation of a fungal mantle.

We next performed a microscopic analysis of the ingrowth of *P. microcarpus* into the root apoplastic space treated with the different synthetic sRNAs (i.e., the formation of the "Hartig net" across whose surface area contact with the plant cells nutrients are exchanged; Fig. 3*B*). We focused on sections of roots that exhibited a mantle and found that no treatment consistently halted the ingrowth of *P. microcarpus* into the root apoplastic space (Fig. 3 *B–H*). However, significant treatment effects were observed on the degree of fungal penetration. Supplementation of *Pmic_miR-8* resulted in a significant increase in Hartig net depth when compared to control-treated tissues (Fig. 3*I*; $P < 0.05$). Conversely, inhibition of *Pmic_miR-8* resulted in significantly less well-developed Hartig nets in the roots analyzed (Fig. 3*I*; $P < 0.05$).

***Pmic_miR-8* Shows Complementarity to Host NB-ARC Domain-Containing Transcripts.** To elucidate the putative pathway(s) in the host plant targeted by *Pmic_miR-8*, further in silico analyses were performed on a complementary set of RNA-seq data that was generated using the same tissues as for sRNA-seq along the ECM colonization timeline in *E. grandis*. Using target prediction based on sequence complementarity and correlation analysis, we identified seven genes on the *E. grandis* genome as potential targets of *Pmic_miR-8* (expectation value <3; Dataset S4) with three highly likely targets (Table 2). These latter targets are orthologous to genes related to DNA endonucleases, protein kinases, and an NB-ARC–containing protein in *Arabidopsis*. A similar analysis was run to identify putative targets within the fungus, but no sequence loci were identified with an appropriate expectation value (i.e., no hits <3; Dataset S5). Similar to *Pmic_miR-8*, *Pmic_miR-3* had a putative *E. grandis* target transcript, while the other secreted miRNAs did not (i.e., *Pmic_miR-2* and *Pmic_miR-9*; Dataset S4). Our analyses identified 19 potential targets endogenous to the fungal genome for these four miRNAs (Dataset S5). We also sought to identify the potential targets of the other *Pisolithus* miRNAs in both the host and fungal genomes (Datasets S4 and S5). For the nonsecreted miRNA *Pmic_miR-1*, *Pmic-miR-6*, *Pmic-miR-7*, *Pmic-miR-10*, and *Pmic-miR-11*, we identified very few endogenous target sequences (Dataset S5) while we were able to isolate several putative target sequences in the *E. grandis* genome (Dataset S4).

To identify the most likely target host gene regulated by *Pmic_miR-8* from the Plant Small RNA Target Analysis Server (psRNATarget) predictions, we performed expression profiling of the three best scoring host target genes (*Eucgr.K00246*, *Eucgr.L01882*, and *Eucgr.E03170*; Table 2) in colonized roots treated with synthetic sRNA as outlined in the previous section. Typically, miRNAs function by reducing the expression of their target genes. Therefore, we expected that roots treated with synthetic *Pmic_miR-8* would exhibit significant reductions in the target transcript with the opposing pattern in roots treated with the *Pmic_miR-8* inhibitors. While this general pattern was observed in all three *E. grandis* genes tested, the pattern was strongest for *Eucgr.E03170*, with significant alterations in all treatments (Fig. 3*J*). This latter gene encodes conserved domains consistent with the CC nucleotide binding and leucine-rich repeat domain immune receptors (CC-NLR) class of proteins. These domains included an Rx N-terminal domain (PFAM 18,052; amino acids 3 to 91), an NB-ARC domain (amino acids 165 to 395), as well as a C-terminal LRR domain (amino acids 554 to 677). A BLASTn search found that there were other *E. grandis* genes encoding a sequence homologous to that found in *Eucgr.E03170* that is likely to be targeted by *Pmic_miR-8*. qPCR analysis demonstrated that the expression of these genes was also influenced by the different treatments with *Pmic_miR-8* inhibitors, with the most consistently significant impact on the expression of *Eucgr.E03196* (Fig. 3*K* and *SI Appendix*, Fig. S4*B*). Therefore, it would appear that *Pmic_miR-8* has the ability to target a number of genes within the largest class of NLRs in plants (30).

Discussion

There is strong support for the possibility of cross-kingdom RNA interference regulating host interactions with pathogenic (21–23) and mutualistic microbes (2, 8, 26, 27, 31, 32). However, we are only beginning to understand miRNAs and their roles in ECM symbioses. This is partly because of the incompatibility of ECM colonization with common model plant species, such as *Arabidopsis* and legumes. ECM fungi interact with the majority of woody plant species in boreal and temperate forests and are key players in soil nutrient cycling in forests globally, where they scavenge/alter soil organic matter and provide vital nutrients to their hosts (13, 33). Studying the role of miRNAs during the development of mycorrhizal roots will deepen our understanding concerning the regulatory pathways vital for this quintessential interaction. Our study provides evidence supporting the significant involvement of fungal miRNA pathways in ECM colonization of the model host plant *E. grandis*. Specifically, like pathogenic fungi, we provide evidence that ECM miRNAs can transfer from the fungus into host cells and

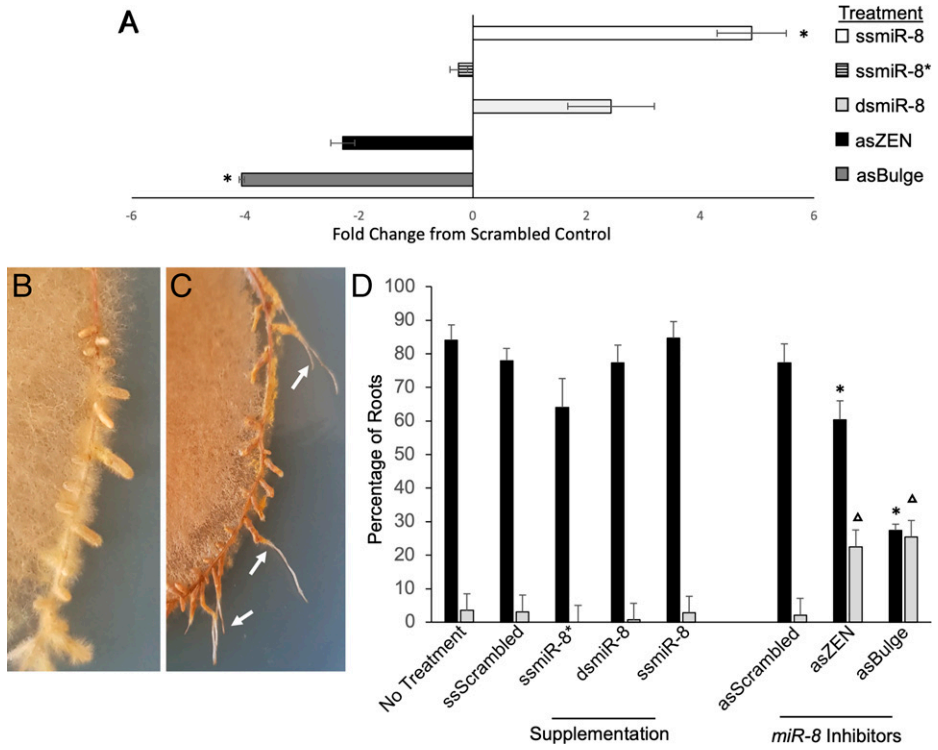

Fig. 2. Supplementation and inhibition of *P. microcarpus miR-8* alters colonization of *E. grandis* roots. (*A*) Relative *Pmic_miR-8* levels in *E. grandis* mycorrhizal root tips treated with either mature, single-stranded *Pmic_miR-8* (white bar), mature as *Pmic_miR-8** (striped bar), or ds *Pmic_miR-8* (light gray bar), as compared to treatment with a scrambled miRNA. We also tested *E. grandis* mycorrhizal root tips treated with either a single-stranded ZEN-tagged as *Pmic_miR-8* inhibitor (i.e., repression; black bar) or a single-stranded as *Pmic_miR-8* with designed bulge mismatch at nucleotides 10 to 11 (dark gray bar), as compared to a scrambled inhibitor sequence. All values are the result of three biological replicates, ±SE; * indicates significant difference from scrambled control ($P < 0.05$; Student's *t* test). (*B*) Representative image of *P. microcarpus* mycorrhizal root tips on *E. grandis* showing a typical mycorrhizal phenotype. (*C*) Representative image of *P. microcarpus* mycorrhizal root tips on *E. grandis* treated with the *Pmic_miR-8* inhibitor in the final week of fungal colonization. White arrows indicate mycorrhizal root tips that have senesced, and the root has recommenced growth. (*D*) Percent of *E. grandis* root tips in contact with *P. microcarpus* that are either colonized by the fungus (black bars) or that exhibit the beginning of colonization followed by senescence (light gray bars). Values are shown for either no spray treatment (No Treatment) or spray treated with scrambled miRNA (ssScrambled); as single-stranded, mature *Pmic_miR-8* (ssmiR-8*); sense ds, mature *Pmic_miR-8* (dsmiR-8); sense single-stranded, mature *Pmic_miR-8* (ssmiR-8); scrambled as inhibitor (asScrambled); single-stranded, ZEN-tagged as *Pmic_miR-8* inhibitor (asZEN); and single-stranded as *Pmic_miR-8* with designed bulge mismatch at nucleotides 10 to 11 (asBulge). All values are based on six biological replicates, ±SE; */△ indicates significant difference from scrambled control ($P < 0.05$; Student's *t* test).

that they act in a manner that stabilizes the colonization of the fungus within root tissues.

While fungal genomes encode a large number of sRNAs, the proportion of these classified as miRNAs are typically in the minority. In the two mutualistic AM genomes analyzed to date, of 702 to 3,422 predicted sRNA loci located in intragenic spaces, 10 miRNAs were annotated within the *R. irregularis* genome and one miRNA was annotated to the *Gigaspora margarita* genome (8, 27). Our discovery of 11 miRNAs within the genome of *P. microcarpus*, therefore, is a comparable number of sequences. Despite only a small number having been functionally characterized, a growing body of research supports the concept of s/miRNA trafficking between fungi and their host during symbiosis. sRNA secreted by fungi directly modulate host physiology to support the colonization process (21–23). While these previous studies have been in pathogenic fungi, our current work has now demonstrated that cross-kingdom sRNA trafficking occurs between ECM fungi and their plant hosts. sRNA-seq analyses identified four fungal miRNAs along with thousands other fungal, siRNA-like RNAs in *E. grandis* roots after presymbiotic interaction. The expression pattern of one of these miRNAs, *Pmic_miR-8*, during the later stages of interaction was similar to that of *Botrytis cinerea* small RNAs (Bc-sRNAs), which transfer from pathogenic *B. cinerea* to *Arabidopsis* (21). This implies that the expression of *Pmic-miR-8* is inducible by the infection event and that it potentially plays a role in the later stage of mycorrhizal fungus–root interaction. Aside from in silico analyses, we conducted ISH assays that further supported the conclusion that *Pmic_miR-8* was not plant derived but exported from *P. microcarpus* into *E. grandis* root cells. ISH assays have previously been used for demonstrating the cross-kingdom transfer of miRNA from plants to human tissue (34). Interestingly, the localization of the miRNA to both the cytoplasm and punctate structures closely mirrors the localization of ARGONAUT proteins (35, 36). Although the pathway is unknown, *Pmic_miR-8* molecules may potentially be transferred through secretion of RNA-containing extracellular vesicles, as has been demonstrated in *Cryptococcus neoformans*, *Paracoccidiodes brasiliensis*, and *Candida albicans* (37).

Typically, exported microbial miRNAs are predicted to suppress host immunity and thus facilitate infection in pathogenic interactions (8, 21–23, 26, 27, 32). This promotional effect on infection was experimentally validated through overexpression of Bc-sRNAs derived from *B. cinerea* and in root colonization of rhizobia when using transfer RNA (tRNA)-derived sRNA fragments (21, 26). Similar to these previous studies, our results indicate that *Pmic_miR-8* stabilizes root colonization during the late stages of colonization, as inhibition of the miRNA led to

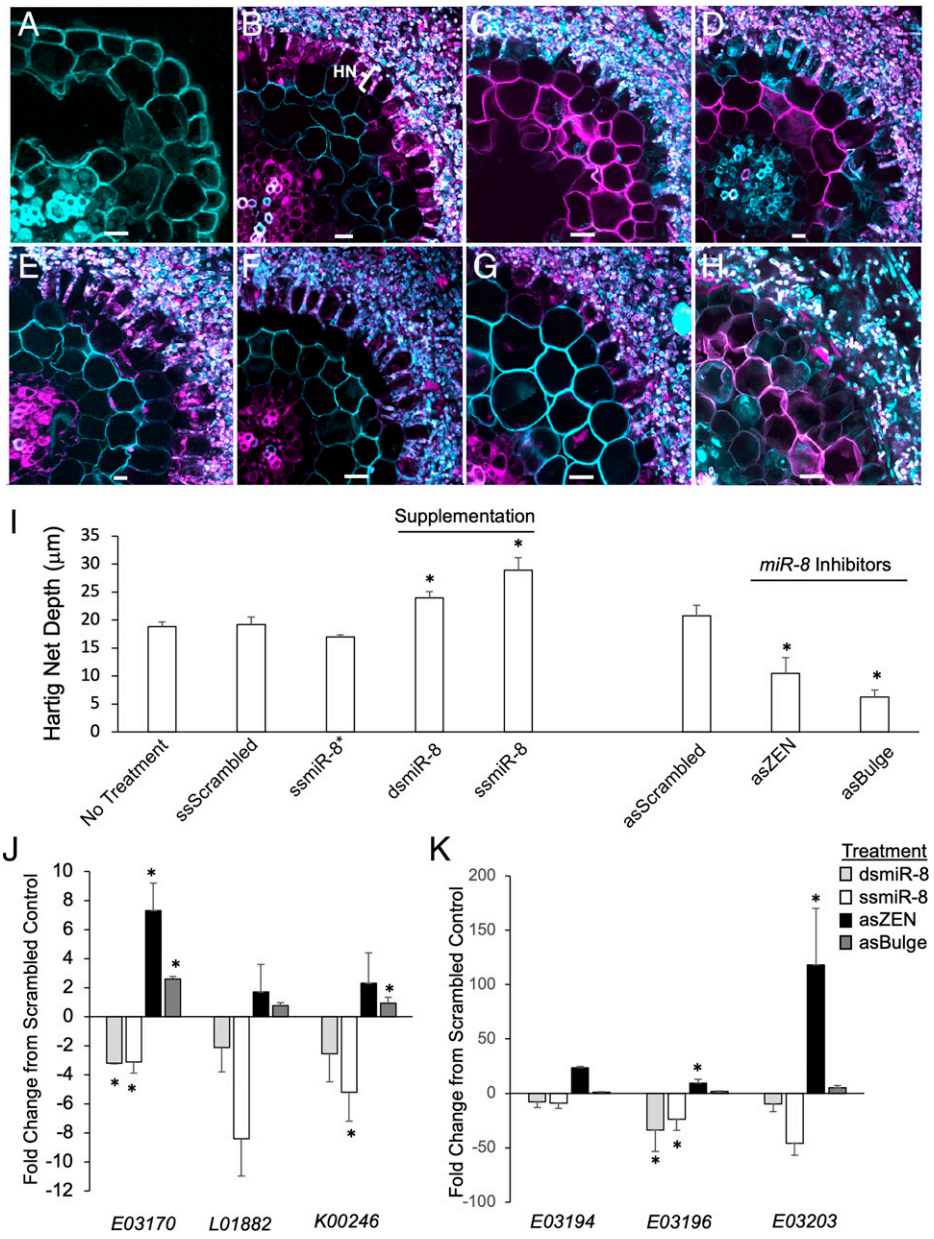

Fig. 3. Supplementation and disruption of *Pmic_miR-8* alters growth of the fungus into the apoplastic space of *E. grandis* roots and expression of host genes. (*A*) Representative transverse cross-section of an axenically grown *E. grandis* lateral root. *P. microcarpus* mycorrhizal root tip on *E. grandis* when sprayed for 1 wk with the following: scrambled control RNA with the Hartig net (HN) penetration marked (*B*); as single-stranded, mature *Pmic_miR-8** (*C*); sense ds, mature *Pmic_miR-8* (*D*); sense single-stranded, mature *Pmic_miR-8* (*E*); scrambled, ZEN-tagged miRNA inhibitor (*F*); single-stranded, ZEN-tagged as *Pmic_miR-8* inhibitor (*G*); and single-stranded as *Pmic_miR-8* with designed bulge mismatch at nucleotides 10 to 11 (*H*). All images are representative of six biological replicates. (Scale bar, 10 μm.) (*I*) Average measured HN depth of *P. microcarpus* in *E. grandis* roots with either no spray treatment (No Treatment) or miRNA sense scrambled (ssScrambled); as single-stranded, mature *Pmic_miR-8** (ssmiR-8*); ds, mature *Pmic_miR-8* (dsmiR-8); sense single-stranded, mature *Pmic_miR-8* (ssmiR-8); scrambled as inhibitor (asScrambled); single-stranded, ZEN-tagged as *Pmic_miR-8* inhibitor (asZEN); and single-stranded as *Pmic_miR-8* with designed bulge mismatch at nucleotides 10 to 11 (asBulge). $n = 6$, ±SE; * indicates significant difference from scrambled control ($P < 0.05$; Student's *t* test). (*J*) qPCR of relative expression of the top three putative *Pmic_miR-8*–targeted gene transcripts (based on in silico prediction) in *E. grandis* mycorrhizal root tips either treated with sense ds, mature *Pmic_miR-8* (light gray bars); sense single-stranded, mature *Pmic_miR-8* (white bars); single-stranded, ZEN-tagged as *Pmic_miR-8* inhibitor (black bars); and single-stranded as *Pmic_miR-8* with designed bulge mismatch at nucleotides 10 to 11 (dark gray bars). $n = 3 \pm$ SE. (*K*) qPCR of relative expression of three putative *Pmic_miR-8*–targeted gene transcripts (based on homology to *Eucgr.E03170*) in *E. grandis* mycorrhizal root tips treated and colored as in *J*. $n = 3 \pm$ SE; * indicates significant difference from scrambled control ($P < 0.05$; Student's *t* test).

the host root escaping the developing, fungal mantle to continue growing. While the full mechanism by which *Pmic_miR-8* achieves this is unknown, one potential pathway is through the modulation of transcript abundance of CC-NLR disease resistance proteins, which are most closely related to R proteins RGA4 and RGA2. These proteins are known to be key regulators of plant immunity, as they detect the presence of an invasive fungus through the perception of fungal avirulence proteins. Activation of RGA4- and RGA2-containing proteins during pathogenic interactions leads to plant resistance against

Table 2. Summary of the three most likely host target genes of *Pmic_miR-8* and their annotation of the orthologous gene in *Arabidopsis*

Target gene ID	*Arabidopsis* ortholog	Expect value*	Alignment
Eucgr.K00246	Single-stranded DNA endonuclease family protein	1.5	*Pmic_miR-8* (1) 5' - UAUUCUCUCCUUGACUUCCC - 3' (20) *Eucgr.K00246* (1204) 3' - AUAAGAGAGGAACUUGAGGU - 5' (1185)
Eucgr.L01882	Single-stranded DNA endonuclease family protein	1.5	*Pmic_miR-8* (1) 5' - UAUUCUCUCCUUGACUUCCC - 3' (20) *Eucgr.L01882* (1282) 3' - AUAAGAGAGGAACUUGAGGU - 5' (1263)
Eucgr.E03170	NB-ARC domain-containing disease resistance protein	1.5	*Pmic_miR-8* (1) 5' - UAUUCUCUCCUUGACUUCCC - 3' (20) *Eucgr.E03170* (378) 3' - AUAAGAGAGGGACUAAAGGA - 5' (359)

*The expectation values are an indicator of the similarity between the *Pmic_miR-8* and the target candidate (50). A smaller value indicates a larger similarity and, therefore, a more probable target candidate. The Alignment column graphically presents the complementary base pairing between *Pmic_miR-8* and the target candidate and is indicated by "|," while U:G wobble pairing is indicated by ".". All putative targets with an expectation value <3 can be found in *SI Appendix*, Table S4.

bacterial (38), oomycete (39), and fungal pathogens (40). Therefore, the potential role of *Pmic_miR-8* in the repression of a number of CC-NLR transcripts may be one of the key mechanisms by which *P. microcarpus* colonizes its host. The finding that disease resistance transcripts may be targeted by an ECM fungal miRNA, though, is different from the predicted plant targets of AM fungal miRNAs (8). In this latter study, the gene ontology of host proteins predicted to be affected by miRNAs included serine-type hydrolases and peptidases, as well as genes associated with the host secretory mechanism. Interestingly, we could not identify potential targets of two other secretory miRNAs in *E. grandis* genome (i.e., *Pmic_miR-2* and *Pmic_miR-9*). As *Pisolithus* species have a broad host range, including *Eucalyptus*, *Cistus*, *Quercus*, *Acacia*, and *Pinus* (41, 42), these secreted miRNAs may have regulatory targets in other plant host species. On the other hand, several putative targets were identified in the *E. grandis* genome for fungal miRNAs undetected in *E. grandis* roots in our study condition (e.g., *Pmic_miR-6*). This may indicate that these miRNAs have regulatory roles in supporting symbiosis under different conditions (e.g., abiotic stress). Further work will be needed to determine if this is the case. Taken together, our results suggest that we have only begun to uncover the breadth of plant-based pathways that are modulated by cross-kingdom fungal miRNA signaling.

The interaction between ECM fungi and plants requires a complex mix of signaling compounds, including metabolites (43–45) and protein effectors (16, 17, 19, 20). We now add to this body of knowledge by demonstrating that ECM fungi can also modulate host function through the transfer of sRNA. In the future, it will be critical to broaden these findings to compare the miRNAs of *P. microcarpus* with other species/evolutionary lineages of ECM fungi to identify the key miRNAs essential for ECM symbiosis.

Materials and Methods

Detailed methods can be found in *SI Appendix*. In brief, following the method previously described in Wong et al. (45), *E. grandis* seeds were sterilized, germinated, and placed into symbiotic interaction with four isolates of the model ECM fungal species *P. microcarpus* [isolates SI9, SI14, R4, and R10; (46)] to identify miRNAs. A time course of colonization between *P. microcarpus* isolates SI14 and SI9 and *E. grandis* was used to profile the expression of identified miRNAs over the course of colonization (i.e., 24 h, 48 h, and 2 wk). In addition, a presymbiotic interaction setup was also prepared according to Wong et al. (45). RNA was extracted from six different conditions (E. grandis axenic control, presymbiosis, 24 h, 48 h, 2 wk, and free-living P. microcarpus mycelium) using the ISOLATE II miRNA kit (Bioline). Three to four biological replicates were extracted per condition. The sRNA fractions were sent for sRNA-seq at the Joint Genome Institute (JGI). In total, 42 sRNA libraries were generated and analyzed (Dataset S6).

Using the reference genome of *E. grandis* (47) and *P. microcarpus* 441 (15), ShortStack was run for each sequencing library in order to identify sRNA-producing loci (or "Clusters") and to identify putative miRNA genes de novo (28, 29). The criteria for sRNA cluster and miRNA gene classification are further detailed in *SI Appendix*. Loci classified as miRNA in the single libraries were merged across libraries (again specifying the "–nohp" option in ShortStack). Along with these miRNA loci clusters, sequences of known miRNAs, previously identified in *E. grandis* roots by Lin et al. (48), were identified and removed. Differential expression analysis was done using DESeq [version 1.30.1; (49)]. Heatmaps were generated with the fold change values of differential-expressed miRNAs [log2(fold change)> 1; adjusted *P* value < 0.05] using Heatmapper (50).

E. grandis seedlings were set up into a presymbiotic interaction or left to grow axenically without fungus for 1 wk before being used for ISH. As detailed in *SI Appendix*, root tips were then divided into several treatments, including control, which were fixed immediately upon harvest; RNase treated for 15 min followed by fixation to remove external bound RNA; RNase treated for 15 min followed by fixation and then a secondary treatment with RNase postfixation and permeabilization to remove external and internal bound RNA; and plasmolysed with 1.5 M sucrose to concentrate internal miRNA and then fixed. Following fixation, samples were treated using 20 μg/mL proteinase K and 0.5% Triton-X in TE buffer for 60 min at 37 °C to digest cellular RNases and protein excess and to permeabilize the cells for probe entry. Samples were incubation in 0.2% glycine at room temperature for 5 min to stop protease activity and probed with LNA probe with a fluorophore modification with anti–*Pmic_miR-8* or a scrambled probe as a control (35 μM, sequences detailed in *SI Appendix*, Table S1). Following incubation, the samples were placed through a series of high-stringency washes to remove unbound probes, followed by staining in 0.1% propidium iodide to stain nuclei. Samples were observed using an inverted Leica SP6 confocal microscope.

To test for the impact of varying *Pmic_miR-8* levels on colonization, *E. grandis* seedlings were directly inoculated with SI14 using the setup mentioned previously, and after 7 d, root systems were sprayed with nebulized, synthetic sRNA of different sequences daily for a further 7 d (100 μL 20-nM sRNA solution per plant using MAD Nasal Intranasal Mucosal Atomization Device; Teleflex; sequences found in *SI Appendix*, Table S1). On the 14th day of colonization (seventh day of sRNA treatment), ECM colonization rate was scored, as were the number of senesced mycorrhizal root tips. Hartig net formation was analyzed as previously described (46). Samples were also collected, and RNA transcript quantitation by qPCR (Primers found in Dataset S7) was used to verify that *Pmic_miR-8* was differentially regulated as expected using a stem loop qRT-PCR approach, as described previously (51).

The sequence of *Pmic_miR-8* has been searched against the nucleotide databases for *E. grandis* on National Center for Biotechnology Information (NCBI) using megaBLAST algorithm to confirm that *Pmic_miR-8* is not of plant origin. No matching loci with a high-confidence score to *Pmic_miR-8* were

identified in the *E. grandis* genome but were identified in the *P. microcarpus* genome (Dataset S2). Therefore, we can be confident that this sequence is of fungal origin. Using psRNATarget [version 2.0; (52)], target sequences of *Pmic_miR-8* and other miRNAs were identified within the *E. grandis* transcript library (Phytozome 11, version 297 v2.0) and the *P. microcarpus* 441 transcript library. Transcripts with an "expectation value" <3 are considered as putative target genes. Detailed methodology for this process can be found in *SI Appendix*. To determine which of the putative host gene(s) may be influenced at the transcriptional level by *Pmic_miR-8* treatment, we took the total RNA extracted from *ss/dsPmic_miR-8* or *Pmic_miR-8* inhibitor-treated tissues as described in the previous paragraph, as well as the scrambled controls, and generated cDNA using the Tetro cDNA synthesis kit (Bioline), as per manufacturer's instructions and using only the oligo-dT primer. Using the SensiFAST SYBR no-ROX qPCR kit (Bioline) following manufacturers' instructions, we then analyzed the expression patterns of the top three putative target genes of *Pmic_miR-8* based on in silico analysis (*Eucgr.K00246*, *Eucgr.L01882*, and *Eucgr.E03170*) or three candidates based on homology to *Eucgr.E03170* (*Eucgr.E03194*, *Eucgr.E03196*, and *Eucgr.E03203*). Relative expression was determined using the $2^{-\Delta\Delta CT}$ method, whereby tissues treated with the scrambled sRNA (either scrambled sense or as miRNA) were used as the control tissues for tissues treated with *ss/dsPmic_miR-8* or *Pmic_miR-8* inhibitors, respectively.

Data Availability. Sequencing data have been deposited in Mycocosm (https://mycocosm.jgi.doe.gov/mycocosm/home) and NCBI (https://www.ncbi.nlm.nih.gov/) (accession nos. are provided in Dataset S6).

ACKNOWLEDGMENTS. J.W.- B. would like to thank Western Sydney University for a PhD research scholarship and the Hawkesbury Foundation for the F.G. Swain Award that supported this research study. J.M.P. would like to acknowledge the Australian Research Council for research funding (DE150100408). This research was also supported by the Laboratory of Excellence ARBRE (ANR-11-LABX-0002-01) to F.M.P. The sequencing work conducted by the US Department of Energy (DOE) JGI, a DOE Office of Science User Facility, is supported by the Office of Science of the US DOE under Contract No. DE-AC02-05CH11231. We wish to acknowledge the aid of R. Wuhrer and T. Richardson of the Western Sydney University Advanced Materials Characterisation Facility for aid in imaging and the Western Sydney Confocal Facility for access to equipment. We would also like to acknowledge the New South Wales National Parks and Wildlife Services for approving the collection of the *Pisolithus* fruiting bodies (Scientific License No. S13146).

1. Y.-S. Ku *et al.*, Small RNAs in plant responses to abiotic stresses: Regulatory roles and study methods. *Int. J. Mol. Sci.* **16**, 24532–24554 (2015).
2. J.-M. Couzigou *et al.*, Positive gene regulation by a natural protective miRNA enables arbuscular mycorrhizal symbiosis. *Cell Host Microbe* **21**, 106–112 (2017).
3. B. J. Reinhart, E. G. Weinstein, M. W. Rhoades, B. Bartel, D. P. Bartel, MicroRNAs in plants. *Genes Dev.* **16**, 1616–1626 (2002).
4. Y. Kurihara, Y. Watanabe, *Arabidopsis* micro-RNA biogenesis through Dicer-like 1 protein functions. *Proc. Natl. Acad. Sci. U.S.A.* **101**, 12753–12758 (2004).
5. H. Vaucheret, F. Vazquez, P. Crété, D. P. Bartel, The action of ARGONAUTE1 in the miRNA pathway and its regulation by the miRNA pathway are crucial for plant development. *Genes Dev.* **18**, 1187–1197 (2004).
6. V. Fulci, G. Macino, Quelling: Post-transcriptional gene silencing guided by small RNAs in *Neurospora crassa*. *Curr. Opin. Microbiol.* **10**, 199–203 (2007).
7. V. Raman *et al.*, Physiological stressors and invasive plant infections alter the small RNA transcriptome of the rice blast fungus, *Magnaporthe oryzae*. *BMC Genomics* **14**, 326 (2013).
8. A. Silvestri *et al.*, In silico analysis of fungal small RNA accumulation reveals putative plant mRNA targets in the symbiosis between an arbuscular mycorrhizal fungus and its host plant. *BMC Genomics* **20**, 169 (2019).
9. M. Kemppainen, S. Duplessis, F. Martin, A. G. Pardo, RNA silencing in the model mycorrhizal fungus *Laccaria bicolor*: Gene knock-down of nitrate reductase results in inhibition of symbiosis with *Populus*. *Environ. Microbiol.* **11**, 1878–1896 (2009).
10. F. Martin *et al.*, Périgord black truffle genome uncovers evolutionary origins and mechanisms of symbiosis. *Nature* **464**, 1033–1038 (2010).
11. B. Montanini *et al.*, Non-exhaustive DNA methylation-mediated transposon silencing in the black truffle genome, a complex fungal genome with massive repeat element content. *Genome Biol.* **15**, 411 (2014).
12. V. Raman *et al.*, Small RNA functions are required for growth and development of *Magnaporthe oryzae*. *Mol. Plant Microbe Interact.* **30**, 517–530 (2017).
13. L. Tedersoo *et al.*, Fungal biogeography. Global diversity and geography of soil fungi. *Science* **346**, 1256688 (2014).
14. S. Miyauchi *et al.*, Large-scale genome sequencing of mycorrhizal fungi provides insights into the early evolution of symbiotic traits. *Nat. Commun.* **11**, 5125 (2020).
15. A. Kohler *et al.*, Mycorrhizal Genomics Initiative Consortium, Convergent losses of decay mechanisms and rapid turnover of symbiosis genes in mycorrhizal mutualists. *Nat. Genet.* **47**, 410–415 (2015).
16. C. Pellegrin *et al.*, *Laccaria bicolor* MiSSP8 is a small-secreted protein decisive for the establishment of the ectomycorrhizal symbiosis. *Environ. Microbiol.* **21**, 3765–3779 (2019).
17. H. Kang *et al.*, The small secreted effector protein MiSSP7.6 of *Laccaria bicolor* is required for the establishment of ectomycorrhizal symbiosis. *Environ. Microbiol.* **22**, 1435–1446 (2020).
18. J. M. Plett *et al.*, A secreted effector protein of *Laccaria bicolor* is required for symbiosis development. *Curr. Biol.* **21**, 1197–1203 (2011).
19. J. M. Plett *et al.*, Effector MiSSP7 of the mutualistic fungus *Laccaria bicolor* stabilizes the *Populus* JAZ6 protein and represses jasmonic acid (JA) responsive genes. *Proc. Natl. Acad. Sci. U.S.A.* **111**, 8299–8304 (2014).
20. J. M. Plett *et al.*, Mycorrhizal effector PaMiSSP10b alters polyamine biosynthesis in *Eucalyptus* root cells and promotes root colonization. *New Phytol.* **228**, 712–727 (2020).
21. A. Weiberg *et al.*, Fungal small RNAs suppress plant immunity by hijacking host RNA interference pathways. *Science* **342**, 118–123 (2013).
22. M. Derbyshire, M. Mbengue, M. Barascud, O. Navaud, S. Raffaele, Small RNAs from the plant pathogenic fungus *Sclerotinia sclerotiorum* highlight host candidate genes associated with quantitative disease resistance. *Mol. Plant Pathol.* **20**, 1279–1297 (2019).
23. S. Kusch, L. Frantzeskakis, H. Thieron, R. Panstruga, Small RNAs from cereal powdery mildew pathogens may target host plant genes. *Fungal Biol.* **122**, 1050–1063 (2018).
24. Y. Song, B. P. H. J. Thomma, Host-induced gene silencing compromises *Verticillium* wilt in tomato and *Arabidopsis*. *Mol. Plant Pathol.* **19**, 77–89 (2018).
25. T. Zhang *et al.*, Cotton plants export microRNAs to inhibit virulence gene expression in a fungal pathogen. *Nat. Plants* **2**, 16153 (2016).
26. B. Ren, X. Wang, J. Duan, J. Ma, Rhizobial tRNA-derived small RNAs are signal molecules regulating plant nodulation. *Science* **365**, 919–922 (2019).
27. A. Silvestri *et al.*, Different genetic sources contribute to the small RNA population in the arbuscular mycorrhizal fungus *Gigaspora margarita*. *Front. Microbiol.* **11**, 395 (2020).
28. M. J. Axtell, ShortStack: Comprehensive annotation and quantification of small RNA genes. *RNA* **19**, 740–751 (2013).
29. N. R. Johnson, J. M. Yeoh, C. Coruh, M. J. Axtell, Improved placement of multi-mapping small RNAs. *G3 (Bethesda)* **6**, 2103–2111 (2016).
30. J. Kourelis, T. Sakai, H. Adachi, S. Kamoun, RefPlantNLR is a comprehensive collection of experimentally validated plant disease resistance proteins from the NLR family. *PLoS Biol.* **19**, e3001124 (2021).
31. D. Lauressergues *et al.*, The microRNA miR171h modulates arbuscular mycorrhizal colonization of *Medicago truncatula* by targeting NSP2. *Plant J.* **72**, 512–522 (2012).
32. S.-J. Lee, M. Kong, P. Harrison, M. Hijri, Conserved proteins of the RNA interference system in the arbuscular mycorrhizal fungus *Rhizoglomus irregulare* provide new insight into the evolutionary history of Glomeromycota. *Genome Biol. Evol.* **10**, 328–343 (2018).
33. R. Landeweert, E. Hoffland, R. D. Finlay, T. W. Kuyper, N. van Breemen, Linking plants to rocks: Ectomycorrhizal fungi mobilize nutrients from minerals. *Trends Ecol. Evol.* **16**, 248–254 (2001).
34. A. R. Chin *et al.*, Cross-kingdom inhibition of breast cancer growth by plant *miR159*. *Cell Res.* **26**, 217–228 (2016).
35. A. K. L. Leung, J. M. Calabrese, P. A. Sharp, Quantitative analysis of Argonaute protein reveals microRNA-dependent localization to stress granules. *Proc. Natl. Acad. Sci. U.S.A.* **103**, 18125–18130 (2006).
36. B.Derrien *et al.*, Degradation of the antiviral component ARGONAUTE1 by the autophagy pathway. *Proc. Natl. Acad. Sci. U.S.A.* **109**, 15942–15946 (2012).
37. R. Peres da Silva *et al.*, Extracellular vesicle-mediated export of fungal RNA. *Sci. Rep.* **5**, 7763 (2015).
38. S. Césari *et al.*, The NB-LRR proteins RGA4 and RGA5 interact functionally and physically to confer disease resistance. *EMBO J.* **33**, 1941–1959 (2014).
39. Y.-L. Zhang *et al.*, Characteristic of the pepper CaRGA2 gene in defense responses against *Phytophthora capsici* Leonian. *Int. J. Mol. Sci.* **14**, 8985–9004 (2013).
40. S. Césari *et al.*, The rice resistance protein pair RGA4/RGA5 recognizes the *Magnaporthe oryzae* effectors AVR-Pia and AVR1-CO39 by direct binding. *Plant Cell* **25**, 1463–1481 (2013).
41. F. Martin, J. Díez, B. Dell, C. Delaruelle, Phylogeography of the ectomycorrhizal *Pisolithus* species as inferred from nuclear ribosomal DNA ITS sequences. *New Phytol.* **153**, 345–357 (2002).
42. K. Hosaka, Phylogeography of the genus Pisolithus revisited with some additional taxa from New Caledonia and Japan. *Bull. Natl. Mus. Nat. Sci. Ser. B Bot.*, **35**, 151–167 (2009).
43. F. A. Ditengou, F. Lapeyrie, Hypaphorine from the ectomycorrhizal fungus *Pisolithus tinctorius* counteracts activities of indole-3-acetic acid and ethylene but not synthetic auxins in eucalypt seedlings. *Mol. Plant Microbe Interact.* **13**, 151–158 (2000).
44. H. Lagrange, C. Jay-Allgmand, F. Lapeyrie, Rutin, the phenolglycoside from eucalyptus root exudates, stimulates *Pisolithus* hyphal growth at picomolar concentrations. *New Phytol.* **149**, 349–355 (2001).

45. J. W.-H. Wong *et al.*, The influence of contrasting microbial lifestyles on the pre-symbiotic metabolite responses of *Eucalyptus grandis* roots. *Front. Ecol. Evol.* **7**, 10 (2019).
46. K. L. Plett *et al.*, Intra-species genetic variability drives carbon metabolism and symbiotic host interactions in the ectomycorrhizal fungus *Pisolithus microcarpus. Environ. Microbiol.* **23**, 2004–2020 (2021).
47. A. A. Myburg *et al.*, The genome of *Eucalyptus grandis. Nature* **510**, 356–362 (2014).
48. Z. Lin *et al.*, Identification of novel miRNAs and their target genes in *Eucalyptus grandis. Tree Genet. Genomes* **14**, 60 (2018).
49. M. I. Love, W. Huber, S. Anders, Moderated estimation of fold change and dispersion for RNA-seq data with DESeq2. *Genome Biol.* **15**, 550 (2014).
50. S. Babicki *et al.*, Heatmapper: Web-enabled heat mapping for all. *Nucleic Acids Res.* **44**, W147–W153 (2016).
51. E. Varkonyi-Gasic, R. Wu, M. Wood, E. F. Walton, R. P. Hellens, Protocol: A highly sensitive RT-PCR method for detection and quantification of microRNAs. *Plant Methods* **3**, 12 (2007).
52. X. Dai, P. X. Zhao, psRNATarget: A plant small RNA target analysis server. *Nucleic Acids Res.* **39**, W155–W159 (2011).